The spin nematic state in triangular antiferromagnets

2007 J. Phys.: Condens. Matter 19 145248

(http://iopscience.iop.org/0953-8984/19/14/145248)

IOP PUBLISHING JOURNAL OF PHYSICS: CONDENSED MATTER

J. Phys.: Condens. Matter **19** (2007) 145248 (6pp) doi:10.1088/0953-8984/19/14/145248

The spin nematic state in triangular antiferromagnets

Hirokazu Tsunetsugu and Mitsuhiro Arikawa

Yukawa Institute for Theoretical Physics, Kyoto University, Kitashirakawa Oiwake-cho, Kyoto 606-8502, Japan

Received 12 December 2006
Published 23 March 2007
Online at stacks.iop.org/JPhysCM/19/145248

Abstract

Motivated by the recently discovered triangular magnet $NiGa_2S_4$, we investigated a spin antiferronematic phase in the spin-1 bilinear–biquadratic model. We obtained the energy dispersion of elementary excitations by bosonizing spin operators, and the dynamic and static spin correlations are calculated. Low energy properties of $NiGa_2S_4$ are consistently explained using the scenario of nematic order, including the algebraic temperature dependence of the specific heat $C(T) \sim T^2$ and a finite value of the magnetic susceptibility at zero temperature. We also calculated the rate of relaxation of the nuclear magnetic resonance, and found $T_1^{-1} \propto T^3$, a scaling different from that in the magnetically ordered phase. Some comments are also given on how to identify antiferronematic orders experimentally.

Recently, the triangular antiferromagnet $NiGa_2S_4$ was found to exhibit very exotic low temperature properties [1]. First of all, although the Weiss temperature is about 80 K, the system does not show a magnetic long range order down to the lowest temperature 0.35 K in the measurement, while the specific heat $C(T) \sim T^2$ below 10 K is similar to that for magnetically ordered states in two dimensions. Secondly, the magnetic susceptibility gradually increases with decreasing temperature, and approaches a finite value. Thirdly, a neutron experiment revealed a peak at an incommensurate wavevector $\mathbf{K} \sim (\pi/\sqrt{3}, 0)$. However, this was not a magnetic Bragg peak, and the spin correlation length did not diverge but saturated to about $\xi \sim 20$ Å, only seven lattice units. In this paper, we will examine the possibility of a hidden order that reproduces low temperature properties similar to those in critical spin liquid states [2–4].

For exploring possible order parameters, an important point is that the system can be described as a pure spin model with no spin anisotropy, since Ni^{2+} ions do not have orbital degrees of freedom [1]. Therefore, order parameters should be represented in terms of spin operators. We will investigate the simplest candidate, spin quadrupole moments, $Q^{\mu\mu'} = \frac{1}{2}\langle S^\mu S^{\mu'} + S^{\mu'} S^\mu \rangle - \frac{1}{3} S(S+1)\delta_{\mu\mu'}$, where μ is the spin index, and this also corresponds to nematic order [5–8]. The order parameter $Q^{\mu\nu}$ describes the anisotropy of spin fluctuations, not

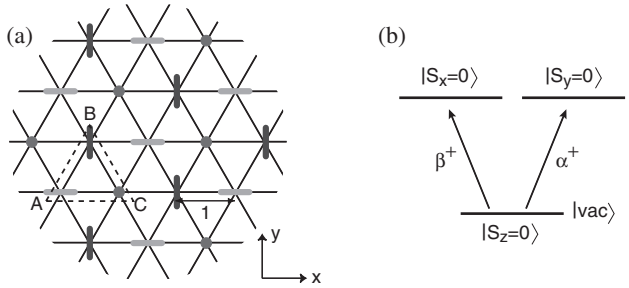

Figure 1. (a) Director configuration of the three-sublattice nematic order. $\mathbf{n}_A \parallel x$, $\mathbf{n}_B \parallel y$, $\mathbf{n}_C \parallel z$. The dotted triangle shows a unit cell of the ordered state. (b) Mean field level scheme in the C-sublattice.

the static moment, and can be nonzero only if $S \geqslant 1$.[1] In $NiGa_2S_4$, local spins are $S = 1$ and therefore we consider the nematic order parameter defined at each site. Neutron experiments revealed a peak of scattering at incommensurate wavevectors $\mathbf{K}$, not at $\mathbf{k} = \mathbf{0}$ or at the Brillouin zone boundary. This suggests that the expected nematic order also modulates in space, i.e., some antiferronematic order.

When nematic orders are explored, the $S = 1$ case is particularly simple. Consider a single-site $S = 1$ system under a general quadrupolar molecular field. We can show that its ground state always has a uniaxial symmetry such that the principal values of $Q^{\mu\nu}$ are two $\frac{1}{3}$ s and one $-\frac{2}{3}$, even when the quadrupolar field is biaxial. Therefore, the axis direction for the smallest principal value is sufficient to characterize the nematic state, and this is called the director $\mathbf{n}$. $-\mathbf{n}$ is equivalent to $\mathbf{n}$. The corresponding wavefunction is given as $(\mathbf{n}\cdot\mathbf{S})|\psi_{\mathbf{n}}\rangle = 0$.

A canonical model describing spin nematic states is the bilinear–biquadratic Hamiltonian, and we will use the $S = 1$ version of this model with nearest-neighbour interactions to investigate the nematic states on the triangular lattice:

$$H = \sum_{\langle \mathbf{r},\mathbf{r}'\rangle} \left[J\mathbf{S}_{\mathbf{r}}\cdot\mathbf{S}_{\mathbf{r}'} + K(\mathbf{S}_{\mathbf{r}}\cdot\mathbf{S}_{\mathbf{r}'})^2 \right]. \tag{1}$$

The mean field analysis for general lattices predicts four types of phase [9, 10]:

(i) ferromagnetic (when $K > J$ and $J < 0$),
(ii) 'antiferromagnetic' (when $K < 0$ and $J > 0$),
(iii) ferronematic (when $K < J < 0$), and finally
(iv) 'antiferronematic' (when $0 < J < K$).

In the ferromagnetic and antiferromagnetic phases, the spin dipole moment has a finite static value, $\langle \mathbf{S}_{\mathbf{r}}\rangle \neq \mathbf{0}$, whereas the quadruple moment is finite, $\langle Q^{\mu\nu}_{\mathbf{r}}\rangle \neq 0$, in the ferronematic and antiferronematic phases. In the antiferromagnetic phase, neighbouring dipole moments 'try' to point in opposite directions, whereas in the antiferronematic phase, neighbouring directors tend to be orthogonal to each other.

It is interesting that the triangular lattice, being tripartite, is not frustrated for the antiferronematic order, since up to three directors can be orthogonal to each other. See figure 1(a). The mean field ground state is unique aside from the trivial degeneracy related to global spin rotation, $|\Psi_{\mathrm{MF}}\rangle = \prod_{\mathbf{R}} |S_x = 0\rangle_{A,\mathbf{R}} \otimes |S_y = 0\rangle_{B,\mathbf{R}} \otimes |S_z = 0\rangle_{C,\mathbf{R}}$. Here, $\mathbf{r} = (j, \mathbf{R})$, with sublattice index $j \in \{A, B, C\}$ and unit-cell coordinate $\mathbf{R}$.

[1] One can also define similar nematic order parameters for spin-1/2 systems, if we compose the effective spin $S \geqslant 1$ using multiple spins with $S = 1/2$.

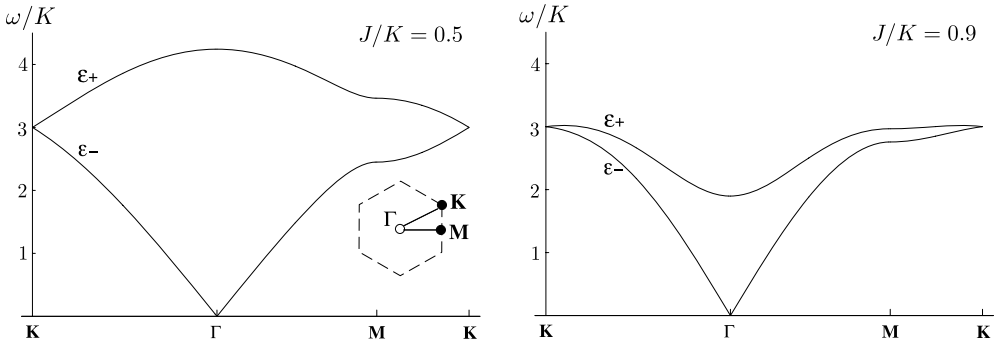

Figure 2. Energy dispersion of two types of excitation for $J/K = 0.5$ and 0.9. The Brillouin zone of the three-sublattice order is also shown. Γ: (0, 0), K: $(2\pi/3, 2\pi/3\sqrt{3})$, M: $(2\pi/3, 0)$.

We now study the effects of quantum fluctuations. To this end, let us represent at each site the local mean field state as a vacuum and the other basis states in terms of two types of boson [7]. For example, in the C-sublattice, $|S_z = 0\rangle = |\mathrm{vac}\rangle$, $|S_z = \pm 1\rangle = (1/\sqrt{2})(\alpha^\dagger \pm \mathrm{i}\beta^\dagger)|\mathrm{vac}\rangle$, and therefore the spin operators are represented as $S^x = \alpha^\dagger + \alpha$, $S^y = \beta^\dagger + \beta$, and $S^z = -\mathrm{i}(\alpha^\dagger\beta - \beta^\dagger\alpha)$, see figure 1(b). In a similar way, α and β bosons are also introduced for the A- and B-sublattices. It is noted that these bosons are subject to the local constraint that at most only one boson can be excited at any site.

We rewrite the model (1) in terms of these boson operators and then neglect their interactions. Then, the Hamiltonian reads in Fourier representation as $H_\mathrm{b} = 3K\Omega + 3K\sum_{\mathbf{k}}[h_{\mathbf{k}}(\beta_A, \alpha_B) + h_{\mathbf{k}}(\beta_B, \alpha_C) + h_{\mathbf{k}}(\beta_C, \alpha_A)]$ and

$$h_{\mathbf{k}}(\beta_j, \alpha_{j'}) = \beta^\dagger_{j\mathbf{k}}\beta_{j\mathbf{k}} + \alpha^\dagger_{j'\mathbf{k}}\alpha_{j'\mathbf{k}} + \tfrac{1}{2}\gamma_{\mathbf{k}}\left\{\left[-(1+\kappa)\beta^\dagger_{j\mathbf{k}}\alpha_{j'\mathbf{k}} + (1-\kappa)\beta^\dagger_{j\mathbf{k}}\alpha^\dagger_{j'-\mathbf{k}}\right] + \mathrm{h.c.}\right\}, \tag{2}$$

where $\kappa = 1 - 2J/K$, Ω is the number of unit cells and the sum is taken over the reduced Brillouin zone of the three-sublattice order, and $\gamma_{\mathbf{k}} = \frac{1}{3}\mathrm{e}^{-\mathrm{i}k_x} + \frac{2}{3}\mathrm{e}^{\mathrm{i}k_x/2}\cos(\sqrt{3}k_y/2) \equiv \Gamma_{\mathbf{k}}\mathrm{e}^{\mathrm{i}\phi_{\mathbf{k}}}$. We can easily diagonalize the boson Hamiltonian by Bogoliubov transformation: $H_\mathrm{b} = \sum_{\mathbf{k},j,m=\pm}\varepsilon_{m,\mathbf{k}}b^\dagger_{jm\mathbf{k}}b_{jm\mathbf{k}} + E_0$ with the eigenenergy

$$\varepsilon_{\pm,\mathbf{k}} = 3K\sqrt{(1 \pm \Gamma_{\mathbf{k}})(1 \pm \kappa\Gamma_{\mathbf{k}})}. \tag{3}$$

The energy dispersion is plotted in figure 2 for $J/K = 0.5$ and 0.9. The ε_- branch is a gapless excitation with asymptotically linear dispersion, $\varepsilon_{-,\mathbf{k}} \sim v\,|\mathbf{k}|$ around $\mathbf{k} = \mathbf{0}$, and the velocity is $v = 3\sqrt{JK/2}$. The ε_+ branch is gapped excitation, and it touches the ε_- branch at energy $3K$ on the six corners of the Brillouin zone. These bosonic excitations contribute to magnetic fluctuations, and therefore, we may call them *magnons* also in this case.

The dynamical spin structure factor is given at zero temperature by $S^{\mu\mu'}_{jj'}(\mathbf{k}, \omega) = \sum_\nu \langle 0|S^\mu_{j,-\mathbf{k}}|\nu\rangle\langle\nu|S^{\mu'}_{j',\mathbf{k}}|0\rangle\delta(\omega - E_\nu + E_0)$, where $|\nu\rangle$ is the eigenstate with energy E_ν and $|0\rangle$ is the ground state. $S^\mu_{j,\mathbf{k}}$ is the Fourier transform of the spin on the j-sublattice. Structure factor $S^{\mu\mu'}_{jj'}(\mathbf{k}, \omega)$ vanishes when $\mu \neq \mu'$. $\bar{S}(\mathbf{k}, \omega) \equiv \sum_j S^{\mu\mu}_{jj}(\mathbf{k}, \omega)$ is isotropic in spin space and obtained as

$$\bar{S}(\mathbf{k}, \omega) = \sum_{m=\pm}\mathrm{e}^{2\theta_{m,\mathbf{k}}}\delta(\omega - \varepsilon_{m,\mathbf{k}}), + \frac{1}{4\Omega}\sum_{\mathbf{q},m,m'=\pm}\sinh^2(\theta_{m,\mathbf{k}+\mathbf{q}} - \theta_{m',\mathbf{q}})\delta(\omega - \varepsilon_{m,\mathbf{k}+\mathbf{q}} - \varepsilon_{m',\mathbf{q}}), \tag{4}$$

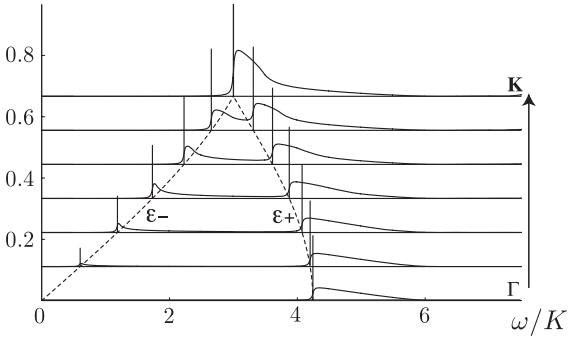

Figure 3. Dynamical spin structure factor $\bar{S}(\mathbf{k}, \omega)$ for $J/K = 0.5$ at $\mathbf{k}$: $\Gamma \to M$. The energy dispersion of $\varepsilon_{\pm,\mathbf{k}}$ is also plotted.

where $e^{4m\theta_{m,\mathbf{k}}} = (1+m\kappa\Gamma_{\mathbf{k}})/(1+m\Gamma_{\mathbf{k}})$. The first and second terms are the contributions of the one- and two-magnon creation processes, respectively. Figure 3 shows $\bar{S}(\mathbf{k}, \omega)$ for $J/K = 0.5$ along the $\Gamma \to$ K direction in the Brillouin zone. For each $\mathbf{k}$, there are two delta-function peaks at the one-magnon energies $\varepsilon_{\pm,\mathbf{k}}$, and they are accompanied by a two-magnon continuum mainly on the higher energy side. As $\mathbf{k} \to \mathbf{0}$, the delta-function peak of the gapless branch vanishes as $\sqrt{K/(8J)}|\mathbf{k}|\delta(\omega - \varepsilon_{-,\mathbf{k}})$. There are no magnetic Bragg peaks, consistent with the absence of ordinary magnetic dipole order.

The magnetic susceptibility χ_m can be calculated from the dynamical correlation function using the relation $\chi_m = \lim_{\mathbf{k}\to\mathbf{0}} \frac{2}{3} \sum_{j,j'\in\{A,B,C\}} \int_0^\infty d\omega\, S^{\mu\mu}_{jj'}(\mathbf{k}, \omega)/\omega$. As $\mathbf{k} \to \mathbf{0}$, the one-magnon contribution of the gapped mode vanishes but that of the gapless mode converges to a finite value, $2/(9J)$. Adding the two-magnon contribution, the result at zero temperature is

$$\chi_m = \frac{2}{9J} + \frac{1}{3\Omega} \sum_{\mathbf{q}} \frac{\sinh^2(\theta_{+,\mathbf{q}} - \theta_{-,\mathbf{q}})}{\varepsilon_{+,\mathbf{q}} + \varepsilon_{-,\mathbf{q}}}, \tag{5}$$

in physical units $(g\mu_B)^2$. It is noted that χ_m is isotropic in spin space. The one-magnon part agrees with the mean field value, and also coincides with the mean field value for the 120-degree order in the pure Heisenberg model. χ_m is dominated by the one-magnon part and the two-magnon part is very small, about 1.85% at largest. In both the $J = 0$ and $J = K$ cases, the two-magnon part of χ_m vanishes, and is $\propto J$ around $J = 0$ and $\propto\sqrt{K - J}$ around $J = K$.

Another important quantity characterizing magnetic properties is the rate of relaxation T_1^{-1} of the nuclear magnetic resonance (NMR). We calculate this following the standard formula [11] $T_1^{-1} = (2A^2/\Omega) \sum_{\mathbf{k}} \bar{S}(\mathbf{k}, \omega_N \to 0+)$. Here, A is a constant determined from hyperfine coupling, and we have neglected its dependence on $\mathbf{k}$. The resonance frequency ω_N is set to be negligibly small. We have calculated the temperature dependence of T_1^{-1} by assuming that thermally excited magnons are not interacting with each other. The result is shown in figure 4 for several values of J/K. The main contribution comes from scattering processes of gapless magnons, predominant over other processes like magnon absorption/emission or those involving gapped magnons. This gives the low temperature asymptotic form,

$$T_1^{-1} = \left(\frac{3A}{8v^2}\right)^2 T^3 + \cdots, \qquad (v = \sqrt{9JK/2}). \tag{6}$$

It is important that this differs from the behaviour in the antiferromagnetically ordered phase $T_1^{-1} \sim T^{2d-3}$ (d: spatial dimension) [11]. Magnetically ordered states have much larger relaxation rate $T_1^{-1} \sim T^1$ in two dimensions. Therefore, the combination of $C(T)$ and $T_1^{-1}(T)$ may be a good experimental test that can identify nematic states.

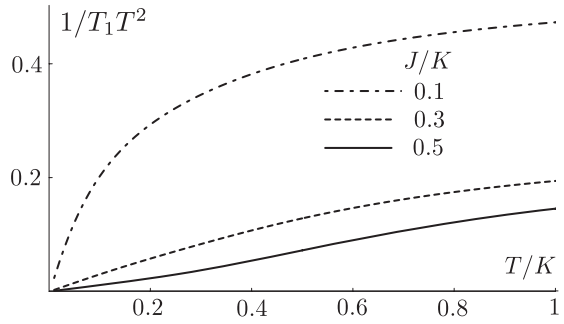

Figure 4. Temperature dependence of the NMR relaxation rate T_1^{-1}. The units are $A^2 = 1$.

Let us summarize the above results and compare with the experiments for $NiGa_2S_4$ [1]. We have found gapless bosonic excitations with linear energy dispersion. They are Goldstone modes owing to the spontaneous breaking of the spin rotation symmetry, since spin fluctuations are anisotropic in the nematic state. The gapless mode contributes to the specific heat as $C(T) \sim 12\pi\zeta(3)(T/v)^2 \sim 45.3(T/v)^2$ in units of k_B per spin. Since the order parameter is a tensor with continuous degrees of freedom as for the 120-degree magnetic order [12], the nematic order does not appear at finite temperatures in two-dimensional systems [13]. However, the spin correlation length grows very rapidly at low temperatures and exceeds the thermal length [14], $\xi \gg L_{\rm th} \sim v/T$. This means that the system is still well ordered up to the length scale where thermal fluctuations matter, and this justifies our calculation assuming a long range order. The zero-temperature magnetic susceptibility is finite and given by $\chi_m \sim 2/(9J)$ plus a tiny quantum correction. The spin structure factor does not show magnetic Bragg peaks, and this is consistent with the neutron experiment. These behaviours agree with the experimental data.

A new result is the calculation of NMR relaxation rate. Our prediction for the antiferronematic state is $T_1^{-1} \sim T^3$. This is considerably suppressed compared with the behaviour in the antiferromagnetic phase in two dimensions, $T_1^{-1} \sim T$, and is rather similar to that of the antiferromagnetically ordered phase in three dimensions. This is because, as discussed for $S(\mathbf{k}, \omega)$, the matrix elements of spin operators between the ground state and low energy excited states have only small amplitude in the nematic phase. Thus, a two-dimensional nematic state looks like a two-dimensional antiferromagnetic state as far as the behaviours of the specific heat and magnetic susceptibility are concerned, while the behaviour is similar to that of a three-dimensional antiferromagnetic state as regards the NMR relaxation rate. When the magnon interaction becomes important at finite temperatures, the above temperature dependence may eventually change to having a renormalized exponent. Although we need more elaborate calculation to take account of effects, it should hold that the nematic state has a larger exponent compared with magnetically ordered states, since low energy magnetic dipole fluctuations are suppressed. In this way, the NMR experiments provide very important information for identifying nematic states and distinguishing them from magnetically ordered systems.

After our proposal of an antiferronematic scenario, two other groups also studied the triangular bilinear–biquadratic model in order to understand $NiGa_2S_4$ [15, 16]. Both groups also proposed a nematic order, but a ferronematic order, and the ferronematic scenario also reproduces results consistent with the experiments including $C(T) \sim T^2$ and $\chi_m(T \to 0) > 0$. As we discussed in the introduction, we believe that a spatially modulated nematic

configuration can more naturally explain the incommensurate nature of magnetic fluctuations, rather than a uniform nematic configuration with frustrated Heisenberg spin–spin couplings. To clarify which case is realized in the real material, we need further investigation including longer range interactions in the model. However, as pointed in [15, 16], one can try two sets of experimental tests.

The first test is that of the anisotropy of magnetic responses in the ordered state [16]. In the ferronematic state, the spin rotation symmetry is lowered from isotropic down to uniaxial. As regards the crystal structure, it is most likely that the uniaxial direction is perpendicular to two-dimensional crystalline planes. Therefore, it is expected that $|\chi_{cc} - \chi_{aa}|$ is large. On the other hand, the antiferronematic state has macroscopic isotropic symmetry, and therefore the above anisotropic should be quite small. The second test is that of the homogeneity of magnetic responses [15], and this is also related to the anisotropy mentioned above. Spins in nematic states do not respond to a magnetic field if their directors are parallel to the field, as long as the applied field is not so strong. More generally, the response is dependent on the angle between the field and the director. Therefore, if a magnetic field is applied to antiferronematic states, induced magnetic moments distribute in space not uniformly but reflecting the director configuration. The modulated pattern of induced moments, if present, can be detected, for example, using neutron scattering. This effect is most visible when the magnetic field is tuned to be parallel to one of the director directions. In the case of ferronematic orders, magnetic moments are induced uniformly in space. These two sets of experiments are handy tests for checking whether an order is ferronematic or antiferronematic, and it is highly desirable for them to be performed in the near future.

Acknowledgments

The authors thank Satoru Nakatsuji, Tsutomu Momoi, Yusuke Nambu, and Keisuke Totsuka for valuable discussions. Parts of the numerical computations were done at the Supercomputer Centre at the ISSP, University of Tokyo, and YITP in Kyoto University. This work was supported by a Grant-in-Aid for Scientific Research on Priority Areas (No. 17071011) and Scientific Research (No. 16540313) from the Ministry of Education, Culture, Sports, Science and Technology of Japan.

References

[1] Nakatsuji S *et al* 2005 *Science* **309** 1697
[2] Anderson P W 1973 *Mater. Res. Bull.* **8** 153
[3] Fazekas P and Anderson P W 1974 *Phil. Mag.* **30** 423
[4] Some of the results in this paper were already reported in Tsunetsugu H and Arikawa M 2007 *J. Phys. Soc. Japan* **75** 083701
[5] Chen H H and Levy P M 1971 *Phys. Rev. Lett.* **27** 1383
[6] Nauciel-Bloch M, Garma G and Castets A 1972 *Phys. Rev.* B **5** 4603
[7] Matveev V M 1974 *Sov. Phys.—JETP* **38** 813
[8] Andreev A F and Grishchuk I A 1984 *Sov. Phys.—JETP* **60** 267
[9] Papanicolaou N 1986 *Phys. Lett.* **116** 89
[10] Fáth G and Sólyom J 1995 *Phys. Rev.* B **51** 3620
[11] Moriya T 1956 *Prog. Theor. Phys.* **16** 23
[12] Kawamura H and Miyashita S 1984 *J. Phys. Soc. Japan* **53** 4138
[13] Mermin N D and Wagner H 1966 *Phys. Rev. Lett.* **17** 1133
[14] Sachdev S 1999 *Quantum Phase Transitions* (Cambridge: Cambridge University Press)
[15] Läuchli A, Mila F and Penc K 2006 *Phys. Rev. Lett.* **97** 087205 (*Preprint* cond-mat/0605234)
[16] Bhattacharjee S, Shenoy V and Senthil T 2006 *Phys. Rev.* B **74** 092406 (*Preprint* cond-mat/0605277)